scientific reports

Check for updates

OPEN

# Graphene oxide doped polyacrylonitrile-*co*-maleic acid nanofibers for high-performance liquid chromatography determination of amoxicillin and Oxytetracycline in milk

Shaymaa A. Mohamed[1], Waleed Alahmad[1], Ibrahim A. Darwish[2], Mohamed Aly Saad Aly[3,4] & Puttaruksa Varanusupakul[1]✉

**Detecting and quantifying trace amounts of antibiotics like amoxicillin and oxytetracycline in milk and environmental water samples is crucial for public health and environmental monitoring. This research focuses on developing a novel sorbent for solid-phase extraction (SPE) of amoxicillin and oxytetracycline from milk and environmental water samples, using electrospun graphene oxide-doped poly(acrylonitrile-*co*-maleic acid) nanocomposite fibers, followed by high-performance liquid chromatography with diode array detection (HPLC-DAD). The fibers were successfully fabricated and characterized using a suite of techniques: SEM-EDX, FTIR, XRD, BET, XPS, TGA, and Raman spectroscopy. The extraction process was optimized by carefully adjusting parameters like desorption solvent (0.60 mL of 0.2 M HCl in methanol), extraction time (60 min), and sample pH (3) to achieve efficient and reliable extraction. Under optimal conditions, the developed method demonstrated good linearity (5–100 µg/L, $R^2 > 0.9925$), low detection and quantification limits (1.50 µg/L and 5.0 µg/L for amoxicillin and 1.46 µg/L and 4.8 µg/L for oxytetracycline) and high enrichment factor (21 for amoxicillin and 47 for oxytetracycline). The achievable accuracy and precision of the developed sorbent were satisfying, for incidence, relative recovery range of 90.3–106.3% and 87.6–95.9% with RSD range of 1.9–4.3% and 1.1–4.7% for amoxicillin and oxytetracycline, respectively. The method demonstrates reliable and efficient extraction and quantification of antibiotics from two different classes at maximum residue levels, making it suitable for monitoring antibiotic contamination in food and environmental samples, ultimately promoting better public health outcomes.**

**Keywords** Electrospun fibers, Graphene oxide, Polyacrylonitrile-*co*-maleic acid, Solid phase extraction, Amoxicillin, Oxytetracycline, Antibiotics

Antibiotics are a class of antimicrobial substances, either naturally produced or synthetic, used to treat and prevent bacterial infections in humans and animals by killing or inhibiting bacterial growth. In recent years, massive discharges from municipal, hospitals, agricultural, and industrial effluent caused contamination to food and aquatic habitats globally, posing significant environmental and health risks[1,2]. Additionally, antibiotic consumption, whether direct or through unintended exposure, can disrupt the gut microbiome, potentially leading to skin allergies, immunopathological effects (such as increased inflammation), and even mutagenic effects (such as changes in DNA)[3,4]. The Joint Food and Agriculture Organization (FAO)/World Health Organization (WHO) Expert Committee on food additives has recommended the acceptable daily intake (ADI)

[1]Department of Chemistry, Faculty of Science, Chulalongkorn University, Bangkok 10330, Thailand. [2]Department of Pharmaceutical Chemistry, College of Pharmacy, King Saud University, P.O. Box 2457, Riyadh 11451, Saudi Arabia. [3]School of Electrical and Computer Engineering, Georgia Institute of Technology, Atlanta, GA 30332, USA. [4]Department of Electrical and Computer Engineering, Georgia Tech Shenzhen Institute (GTSI), Shenzhen 518055, Guangdong, China. ✉email: puttaruksa.w@chula.ac.th

levels for oxytetracycline and amoxicillin residues to be 30 and 2 μg/kg bw/day, respectively[5]. The antibiotic residues in many foods have been found to exceed the maximum residue levels (MRLs) established by WHO, which raises concerns about potential health risks for consumers[6]. In 2018, a survey of eight farms in Thailand reported a total antibiotic footprint of 101 mg/kg in poultry production. Amoxicillin (AMX) was reported to be the most used antibiotic at a rate of 33 mg/kg, while oxytetracycline (OTC) was utilized at 19 mg/kg[7]. These residues can be transferred to water sources, leading to contamination of both water sources and food products. Therefore, regular monitoring of food and water for antibiotic residues is essential to ensure the safety of the food supply and protect public health, especially in low-income countries where access to safe and nutritious food remains a challenge[8].

Various analytical techniques have been employed to date for the identification of antibiotics, such as capillary electrophoresis (CE), fluorescence, and high-performance liquid chromatography (HPLC)[9]. A range of detectors, such as ultraviolet (UV), tandem mass spectrometry (MS/MS), diode arrays (DAD), and fluorescence (FLD), have been used[10]. Due to the complexity of samples and the significant levels of interference, the determination of trace antibiotics in food and environmental matrices remains fraught with difficulties. Therefore, preparation of samples is often required prior to instrument analysis, which greatly affects the sensitivity and selectivity of the analysis as well as the precision and accuracy[11–13].

Solid phase extraction (SPE) is the most used method for extracting antibiotic contaminants from complex mixtures such as food and water samples[14,15]. It has several advantages, including high preconcentration efficiencies, high reproducibility, minimal organic solvent use, and ease of automation[16,17]. In terms of simplicity, cost-effectiveness, and energy consideration, selective sorbent-based materials have been used in SPE to improve extraction efficiency, such as magnetic nanoparticles (MNPs)[18], graphene oxide (GO), metal-organic frameworks (MOF)[19], molecularly imprinted polymers (MIPs)[20,21], and electrospun nanofibers[22].

Electrospun nanofibers (E-spun NFs) exhibit distinct characteristics, including high surface area-to-volume ratio, high porosity, exceptional mechanical strength, adaptable surface functionalities, and recyclability. These attributes collectively suggest a substantial potential for enhanced performance in SPE-based methods[23,24]. Indeed, electrospinning has been recognized as a key technology with diverse applications extraction processes, tissue engineering, pharmaceutical development, chemical sensing, catalysis, and filtration methods.

To address the limitations of traditional adsorbents in terms of sensitivity, selectivity and interference from complex matrices, the incorporation of nanomaterials such as graphene oxide/graphene quantum dots/reduced graphene oxide has found extensive utility in numerous extraction techniques and nanosensor applications due to its remarkable characteristics[25–27]. These include its large surface area, stability across diverse physicochemical conditions, and exceptional electrochemical properties[28]. GO has high hydrophilicity, allowing it to be a suitable adsorbent for enriching carbon-based rings using long-lived and recyclable materials[29]. Incorporating GO into the polymeric network significantly increases the extraction efficiency of the electrospun sorbent. This enhancement arises from the manifold interactions enabled between GO and the target analytes[30,31]. These interactions include hydrogen bonding, hydrophobic interactions, and π–π stacking, thereby facilitating improved capture and extraction of analytes[32].

Based on the above-mentioned facts, the present study aimed to develop a novel sorbent for the effective and highly accurate solid-phase extraction (SPE) of amoxicillin and oxytetracycline from milk and environmental water samples, using electrospun graphene oxide-doped poly(acrylonitrile-*co*-maleic acid) nanocomposite fibers, followed by high-performance liquid chromatography with diode array detection (HPLC-DAD). The proposed method for detecting antibiotic residues in milk stands out for its simplicity and environmental friendliness, requiring minimal organic solvents in sample pretreatment, which aligns with green analytical chemistry principles.

## Materials and methods

### Materials

*Chemicals*

Amoxicillin (AMX, Alfa Aesar, UK), and oxytetracycline (OTC, Sigma-Aldrich, USA) used in this study were purity grade (≥ 97.0%). Acrylonitrile was purchased from Acros Organics (Netherlands). Maleic anhydride, N, N-dimethyl-formamide (DMF), and acetonitrile (ACN) of HPLC grade were purchased from Merck (Germany). AMX was dissolved in ultrapure water, while OTC was dissolved in methanol at a concentration of 1000 μg/mL and stored at 4 °C. The working standard solutions (0.1–10 μg/mL) were freshly prepared by diluting the stock solutions with Milli-Q water. In order to prevent decomposition of OTC, all solutions were stored in an amber container or wrapped with aluminum foil.

*Instruments*

The electrospinning fibers were prepared using a high-voltage power supply (ARUN3D, Thailand) and a syringe pump (ProSense BV The Netherlands). The chemical structure and morphology were analyzed using Nicolet iS50 Fourier transform infrared spectroscopy (FTIR) and scanning electron microscopy (SEM, JEOL IT-200). The diameter distribution of the nanofibers was determined from the SEM images using ImageJ software. X-ray diffractometry (XRD, Rigaku/Smart LAB) was employed to investigate crystallinity, while Brunauer, Emmett, and Teller analysis (BET, BELPREP2, BelJapan) examined the surface area and pore size distribution of the fabricated nanofibers. For elemental composition and chemical state at the material's surface X-ray photoelectron spectroscopy was performed (XPS, PHI-VersaProbe4), and thermal properties were assessed through thermal gravimetric analysis (TGA, PerkinElmerPyris1). HPLC with a DAD detector (Agilent 1290) was used for quantitative analysis.

*Real samples*

Water samples were collected from the Saen Saep canal (Bangkok, Thailand) and the pond within the Chulalongkorn University campus (Bangkok, Thailand). All water samples were filtered with Whatman® no.1 filter paper and a 0.22 µm syringe filter before the extraction. Milk samples, both skim and whole, were purchased from a local convenience store in Bangkok, Thailand. The milk sample was treated with a few drops of concentrated HCl to precipitate the protein and adjust the pH level of the sample. Then, the milk sample was centrifuged at 5000 rpm and 4 °C for 20 min. The supernatant was separated and subsequently filtered through a 0.22 µm syringe filter prior to extraction with GO-PANCMA NFs.

## Methods

*Synthesis of GO and Poly (acrylonitrile-co-maleic acid)*

The modified Hummers' method was used to prepare GO, following the previously described steps[33]. In brief, graphite flakes (3.0 g, 1 weight equivalent) and $KMnO_4$ (18.0 g, 6 weight equivalent) were added to a concentrated $H_2SO_4$/$H_3PO_4$ mixture (360:40 mL) and stirred at 50 °C for 12 h. Then, the mixture was cooled down to room temperature before adding 3 mL of hydrogen peroxide to the solution, which is done in an ice bath until a yellow color is achieved. The GO solid was separated by centrifugation at 4000 rpm for 10 min and then washed with 30% HCl and Milli-Q water. Finally, the solid was freeze-dried to get GO powder.

Poly(acrylonitrile-*co*-maleic acid) (PANCMA) was synthesized by following the previously described in situ polymerization of acrylonitrile and maleic anhydride[34] with minor modifications. 7.4 g maleic anhydride, 13.3 mL acrylonitrile, and 20 mL Milli-Q water were mixed, and the pH level was adjusted to 2.0 using diluted sulfuric acid. Under the $N_2$ atmosphere, $K_2S_2O_8$ (0.136 g) and $Na_2SO_3$ (0.077 g) were added to the previous mixture and stirred at 60 °C for 3 h. The result polymer was filtered, washed with Milli-Q water and ethanol, and then dried at 60 °C for 12 h.

*Synthesis of GO-PANCMA NFs*

The GO-doped PANCMA nanocomposite fibers were fabricated using an electrospinning technique. First, 3 wt % of PANCMA was dissolved in DMF at 70 °C, while 1 wt % of GO was dispersed in DMF with the assistance of an ultrasonic bath for 20 min. Then, the solutions were mixed and used for electrospinning of GO-PANCMA NFs. The electrospinning conditions were a 25% relative humidity, a 0.2 mL/min flow rate, a 10 cm distance between the syringe tip and collector, and a 15 kV voltage. The obtained nanofibers were dried at 60 °C for 2 h.

*SPE procedure*

The GO-PANCMA NFs (6.0 mg) were placed in a holder and preconditioned by flowing 2.0 mL of methanol followed by 2.0 mL of Milli-Q water through the GO-PANCMA NFs. 10 mL of milk or 50 mL of water samples were then loaded at the rate of 0.83 mL/min. For desorption, 0.6 mL of the desorption solvent (0.2 M HCl in methanol) was applied for 10 min at a flow rate of 0.06 mL/min. The obtained extract was filtered using a 0.22 µm syringe filter before analysis by HPLC-DAD.

*HPLC-DAD analysis*

HPLC analysis was performed on an Agilent HPLC system with an Eclipse XDB- C18 column (4.6 × 150 mm I.D., 3.5 µm particle size). The mobile phase consisted of 0.1% formic acid in ultrapure water (eluent A) and ACN (eluent B). The injection volume was 20 µL with a flow rate of 1 mL/min. Gradient elution mode was utilized to adjust the polarity of the mobile phase as follows: 0–3 min: constant 10% B; 3–7 min: increased from 10 to 40% B; 7–8 min: constant 40% B; 8–9 min: decreased from 40 – 10% B; and 9–10 min: re-equilibrate in 10% B. AMX and OTC were monitored at 230 nm and 270 nm, respectively.

*Extraction recovery and enrichment factor calculations*

The enrichment factor (EF) was calculated using Eq. (1):

$$EF = \frac{C_o}{C_{aq}} \tag{1}$$

where $C_o$ represents the final concentration of the analyte in the organic phase (the desorption solvent), while $C_{aq}$ stands for the initial concentration of the analyte in the aqueous phase.

The extraction recovery (ER%) was calculated using Eq. (2):

$$ER\% = \left(\frac{C_o \times V_o}{C_{aq} \times V_{aq}}\right) \times 100 \tag{2}$$

where $V_o$ represents the volume of the organic solvent, while $V_{aq}$ stands for the volume of the aqueous phase[35].

The relative recovery percentage (RR%), which indicates the method's accuracy obtained from the spiked samples, was calculated using Eq. (3):

$$RR\% = \left[\frac{(C_{found} - C_{real})}{C_{spiked}}\right] \times 100 \tag{3}$$

where $C_{found}$ represents the concentration found in the sample after spiking, $C_{real}$ represents the concentration in the original sample, and $C_{spiked}$ represents the level of spiked concentration.

## Results and discussion

### Characterization of GO-Doped PANCMA NFs

#### *Morphology of GO-Doped PANCMA NFs*

The morphology of PANCMA and GO-PANCMA NFs was investigated using SEM-EDX. The morphology of PANCMA and GO-PANCMA NFs, was smooth and uniform, as shown in Figs. 1**(a)** and **1(b)**, and Figs. 1**(c)** and **1(d)**, respectively. However, the diameter of GO-PANCMA fibers (300 ± 32 nm) was larger than that of PANCMA fibers (188 ± 45 nm). This is due to the increase in the viscosity of the polymer solution after adding GO, reducing the stretch of the polymer solution during electrospinning. In addition, the increase of O%, and the decrease of both C% and N%, observed from EDX data summarized in **Table S1**, confirm the successful doping of GO in PANCMA NFs.

*Structural characterization*

The FTIR analysis of GO, PANCMA NFs, and GO-PANCMA NFs revealed the bonding configuration of the prepared nanocomposite fibers, as shown in Fig. 2**(a)**. The characteristic peaks for the PANCMA were noted at 2920 $cm^{-1}$ (C–H bending vibration), 2250 $cm^{-1}$ (C ≡ N stretching vibration), and 1450 $cm^{-1}$(-CH2 scissoring vibration)[36]. For GO, the characteristic peaks were observed at broadband appearing within the range of 3300–3600 $cm^{-1}$ (–OH stretching), 1730 $cm^{-1}$(C = O stretching vibration), 1620 $cm^{-1}$(C = C stretching vibration), 1260 $cm^{-1}$ (C–OH stretching vibration), and 1060 $cm^{-1}$(C-O-C stretching vibration)[37]. In comparison with the spectra of GO and PANCMA, all characteristic bands were present in the spectrum of GO-PANCMA NFs, indicating the successful incorporation of GO into the PANCMA polymer.

The XRD analysis was utilized to examine the structural purity and crystallinity of the nanofiber membranes. Figure 2**(b)**shows the XRD charts for GO, PANCMA, and the NFs membrane of GO-PANCMA. The distinctive sharp peak of GO appeared at 2θ = 10°. As for PANCMA, the broad peak centered at 2θ = 24.26° is associated with the amorphous phase of pure PANCMA, while the sharp peak at 17.47° corresponds to the orthorhombic PANCMA reflection, aligning with previously reported literature results[28,36]. Successful incorporation of GO into the composite structure is confirmed by all peaks observed in the composite NFs.

The presence of GO in the NFs was confirmed using Raman spectroscopy. The typical Raman spectra of GO, PANCMA, and GO-PANCMA are shown in Fig. 2**(c)**. The production of GO is confirmed by the presence of D and G bands at 1356 and 1591 $cm^{-1}$, respectively. The appearance of D and G bands at 1366 and 1599 $cm^{-1}$for GO-PANCMA NFs indicates the successful GO doping into PANCMA[38]. Furthermore, the shifting of the D and

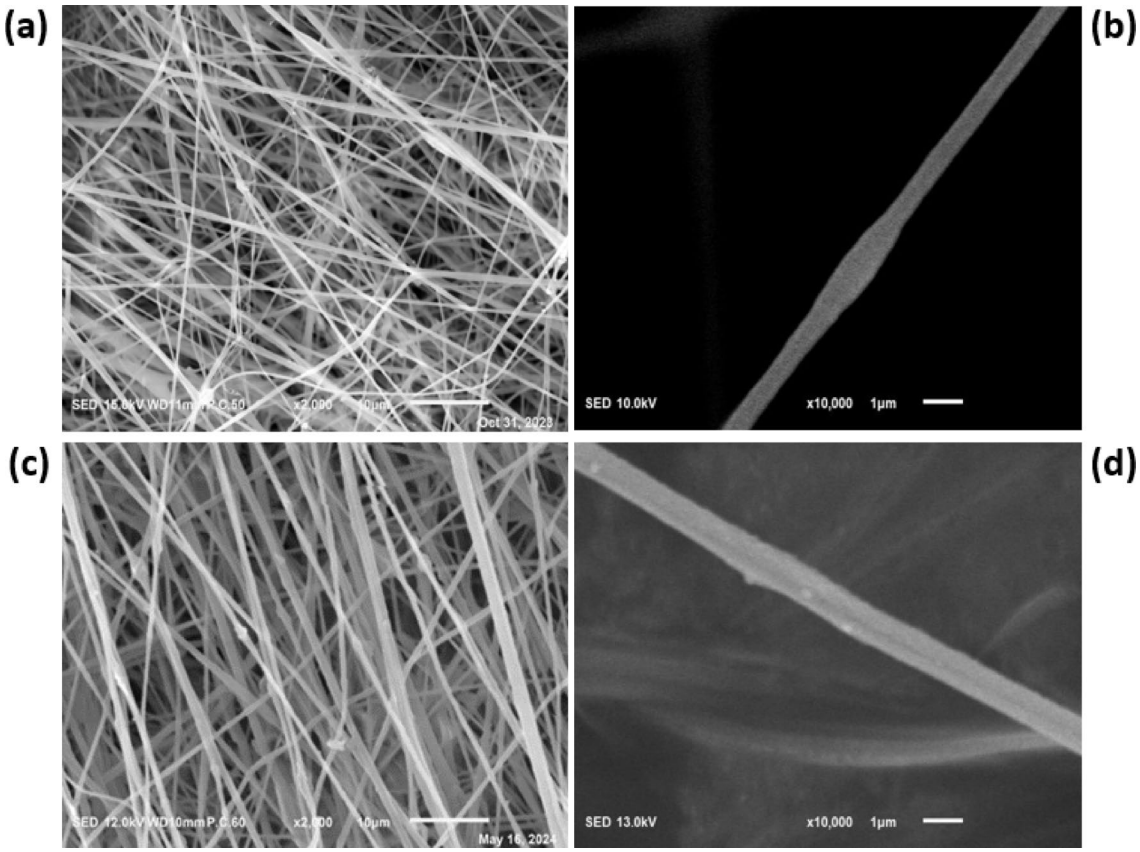


**Fig. 1**. SEM analysis of PANCMA NFs **(a)** and **(b)**, GO-PANCMA NFs **(c)** and **(d)** at 2000x and 10000x, respectively.

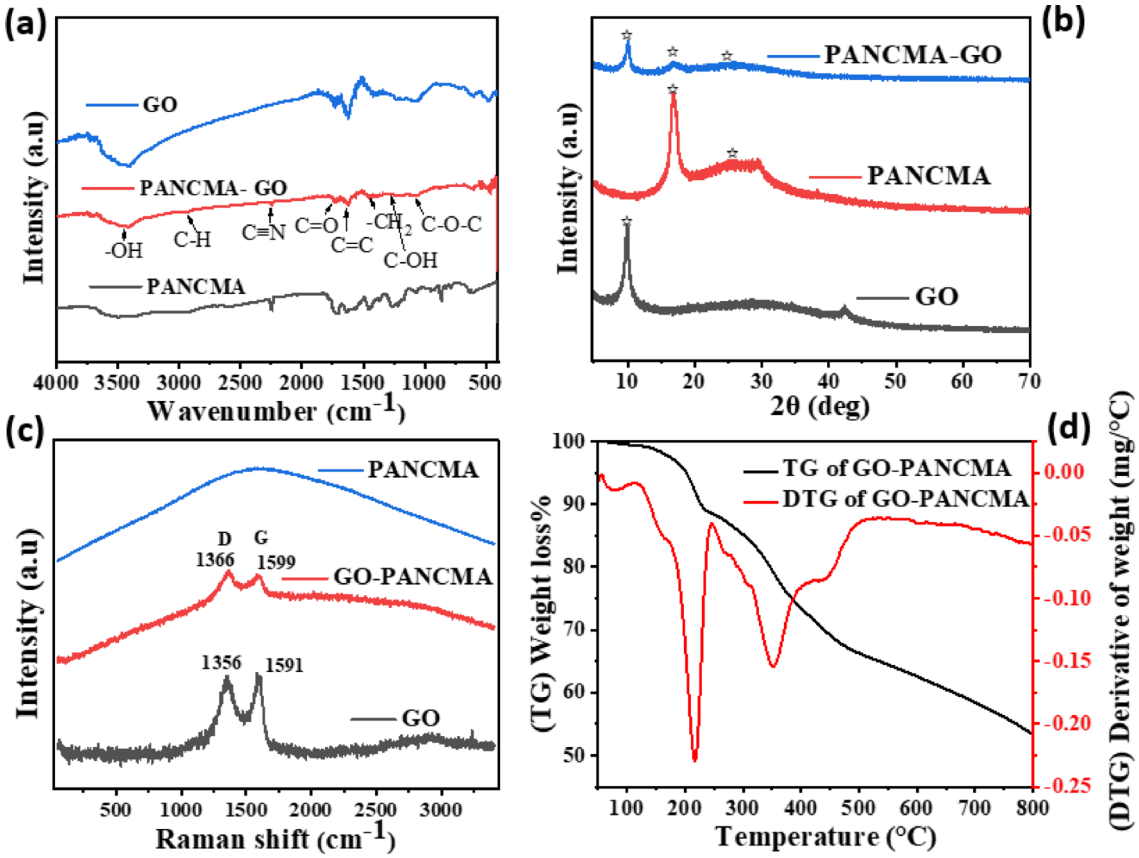


**Fig. 2**. FTIR (**a**), XRD (**b**), Raman spectroscopy (**c**), and TGA (**d**) analysis of PANCMA and GO-PANCMA NFs.

G bands in GO-PANCMA NFs indicates the interaction of GO with PANCMA. The calculated $I_d/I_g$ of GO was found to be 0.85, matching the previously reported data[39].

To investigate the chemical nature of the resultant nanocomposite, XPS was performed on GO-PANCMA NFs, which provided an exact elemental composition in the top 1–12 nm of the sample surface. The XPS wide-scan spectra shown in **Figure S1**confirm the composition of C, O, and N in the GO-PANCMA NFs. The C1 s composition of NFs indicated in the XPS spectra can be divided into four peaks with the binding energy of 284.4 eV (C = C), 285.3 eV (C-C) 286.2 eV (C ≡ N, C-OH), and 287.7 eV (C = O)[40,41]. The N1 s composition of NFs indicated in the XPS spectra consists of one peak with a binding energy of 399.2 eV (N ≡ C). The O1 s composition of NFs indicated in the XPS spectra can be deconvoluted into three peaks with the binding energy of 531.2 eV (O-C), 532.1 eV (O = C), and 533.4 eV (HO-C), which are consistent with the results reveled from the FTIR spectra.

*Thermal gravimetry analysis*

The thermal stability of the produced GO-PANCMA NFs membranes was examined using TGA at a 10 °C $min^{-1}$ scan rate, in an $N_2$ environment, and up to 800 °C. Three stages of weight loss were observed within three distinct temperature ranges, as represented by the TG plot shown in Fig. 2**(d)**. During the first stage, there was a slight decrease in weight which continued up to 200 °C. The physically adsorbed water moieties was dehydrating during this temperature range, thus explain this weight loss. In the second stage, the decarboxylation of nanofibers is responsible for the initial significant weight loss that happened in the second temperature range of 220–340 °C. During the third stage, a significant weight loss happened within the temperature range of 480 to 800 °C. This can be attributed to the thermo-oxidative breakdown of the GO and PANCMA chain. This also agrees with the results previously reported[42,43]. Strong evidence of the two significant weight losses for the sample can also be found in the associated DTG plot, represented by two sharp and intense peaks at 220 and 350 °C. Therefore, It can be concluded that the produced GO-PANCMA NFs are clearly thermally stable below 200 °C.

*Surface area analysis*

The specific surface area and porosity of the prepared GO-PANCMA NFs were examined by $N_2$ adsorption – desorption analysis. By looking at **Figure S2**, it can be concluded that PANCMA NFs resembles type -II isotherm for non-porous adsorbent, with a distinctive flat region in the center signifying the monolayer formation. Furthermore, GO-PANCMA composite nanofibers resembles a type-IV isotherm, confirming the presence of mesoporous material observed within the relative pressure range of 0.3 – 0.97[44,45]. By looking at the

data summarized in **Table S2**, it can be noted that GO-PANCMA NFs showed a larger $S_{BET}$ and pore volume than these of PANCMA NFs. These support that GO-PANCMA NFs are potentially effective in adsorbing antibiotics.

## Extraction performance of GO-PANCMA NFs

As demonstrated in Fig. 3**(a)**, PANCMA NFs were ineffective in extracting AMX and OTC. The extraction recovery of AMX and OTC on PANCMA NFs was 4.5% and 6.4%, respectively. These values are notably lower compared to those observed on the GO-PANCMA NFs (33.7 and 99.8%, respectively) under the same experimental conditions. This significant difference in extraction efficiency suggests that the incorporation of GO enhances the adsorption capabilities of the nanofibers, allowing for more effective capture of the target compounds. GO-PANCMA NFs exhibit adsorption through π–π interaction and cation–π bonding, while PANCMA NFs present only hydrogen bonding interaction. In addition, the % ER of AMX is noticed to be lower than that of OTC because of the difference in polarity of both AMX and OTC. Since the primary component of the created composite is PANCMA (3 weight%), an intrinsically hydrophobic polymer with a lengthy alkyl chain, the adsorption effectiveness of OTC on GO-PANCMA NFs is enhanced because of their similar hydrophobic characteristics[46]. According to the principle of "like dissolves like", AMX, being hydrophilic, has a reduced tendency to interact with the hydrophobic GO-PANCMA NFs.

## Optimization of SPE conditions

The SPE parameters, including type and volume of desorption solvent, extraction time, and sample pH, were studied to obtain the optimal extraction efficiency.

*Effect of desorption solvent*

Several desorption solvents were chosen for the study based on the physicochemical properties of AMX and OTC, including MeOH, 4 M formic acid, 4 M oxalic acid, and 0.2 M HCl in MeOH as shown in Fig. 4**(a)**. The best desorption solvent for AMX and OTC was 0.2 M HCl in MeOH as shown in the results represented in Fig. 4**(a)**. The acidified solvent increases the solubility of analytes in the organic phase by weakening the bonds between analytes and NFs[47]. Both AMX and OTC contain ionizable functional groups that can exist in different charge states depending on the pH level. Under acidic conditions, these molecules become protonated, reducing their affinity for binding to NFs and increasing their solubility in the organic phase, thus improving the desorption efficiency[48].

The volume of the desorption solvent was investigated by varying the volume of the 0.2 M HCl in MeOH from 200 to 800 µL, as presented in Fig. 4**(b)**. The AMX and OTC recoveries increased with an increase in the volume of 0.2 M HCl in MeOH and reached the maximum at 600 µL. Due to the dilution of the analytes extract, a slight decrease in recoveries at the volume of 800 µL. Therefore, the optimum solvent volume to desorb the analytes from the fibers was found to be 600 µL.

*Effect of sample pH*

Analyte adsorption on GO-PANCMA NFs can be affected by the pH level of the sample solution, which is a significant factor influencing the chemical structure of analytes and the surface charge of the adsorbent. The effect of pH was studied in the range of (2–9) and the results are shown in Fig. 4**(c)**. According to the chemical structures and pKa values, the pH affects the form of AMX and OTC [cationic (pH < pKa1), zwitterionic (pKa1

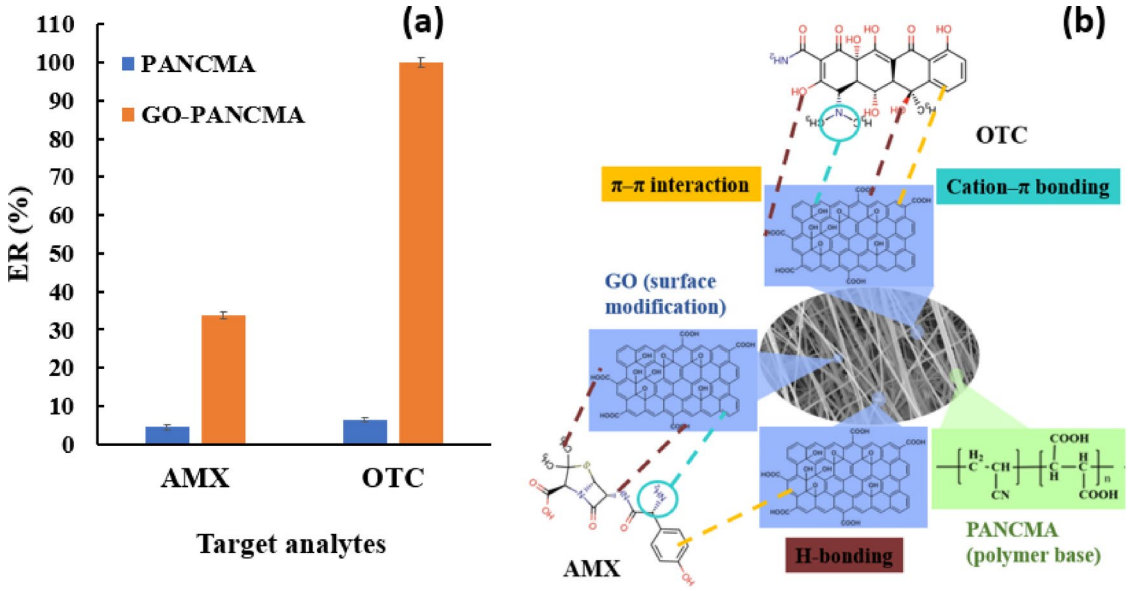


**Fig. 3**. Extraction recovery of AMX and OTC with PANCMA and GO-PANCMA NFs **(a)**, and Possible adsorption mechanism of AMX and OTC by GO-PANCMA NFs **(b)**.

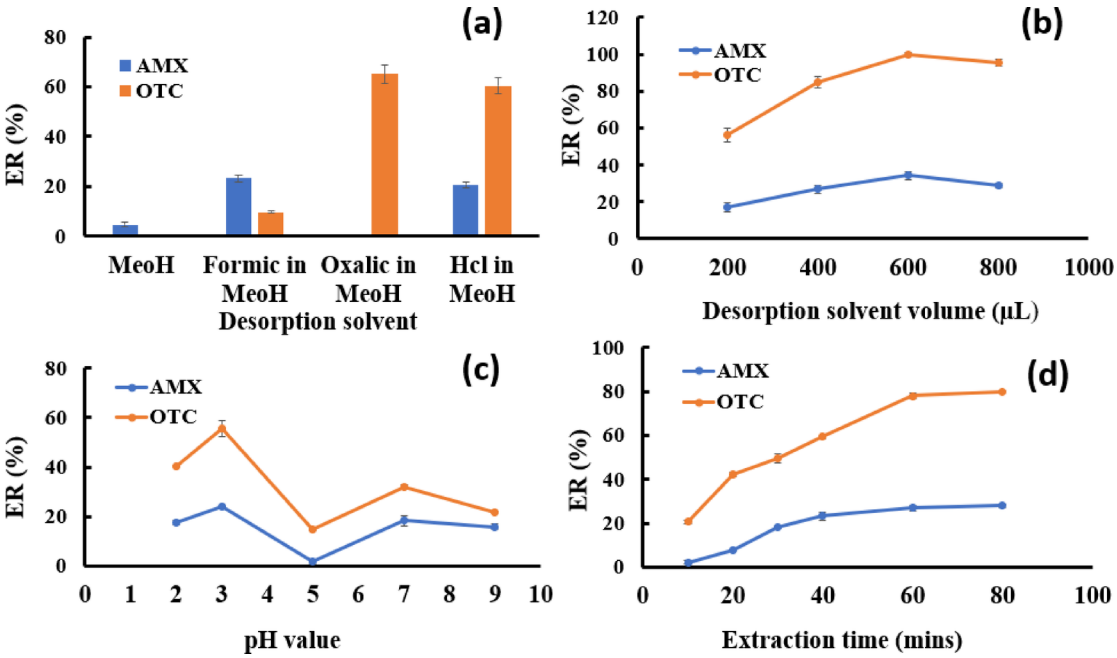


**Fig. 4**. Optimization of SPE parameters: desorption solvent **(a)**, desorption solvent volume **(b)**, sample pH **(c)**, and extraction time **(d)**. Analytes concentration, 50 µg/L; sample volume, 50 mL; flow rate, 0.83 mL/min; sorbent weight, 6 mg.

< pH < pKa3), and anionic (pH > pKa3) forms]. The results revealed that the highest analytical signal was achieved below a pH level of 3, at which AMX and OTC are cationic species, thus they can electrostatically interact with the negative charge on the surface of the developed NFs[49,50]. This is also due to the dominant mechanism, π–π interaction, and cation–π bonding occurring between the GO-PANCMA fibers and AMX and OTC, as shown in Fig. 3**(b)**[51,52]. As a result, the pH level of 3 was chosen as the optimal pH level of sample for extraction.

*Effect of extraction time*

The interaction time between the adsorbent and the sample solution plays a crucial role in the adsorption process. In solid phase extraction, it necessitates a sufficient time for analytes to be retained on a sorbent[53,54]. The effect of extraction time was examined from 10 to 80 min, and the results are depicted in Fig. 4**(d).** For AMX, %ER increased by increasing the extraction time until 40-minutes and reached the equilibrium at 60-minutes, while OTC achieved the optimal % ER at 60-minutes. To compromise the extraction efficiency for both analytes, 60 min was chosen as the extraction time for further analysis.

## Reusability test

The ability to reuse an adsorbent for multiple extraction cycles without a significant loss in performance, reusability, is a key indicator of its cost-effectiveness, as it reduces the need for frequent adsorbent replacement and associated costs. For this study, the 50 mL of water spiked with 50 µg/L AMX and OTC was extracted and desorbed by 0.6 mL of 0.2 M HCl in methanol. The GO-PANCMA NFs were then washed with distilled water and methanol before being used in the next cycle of extraction. The extraction recoveries of analytes in each cycle are illustrated in Fig. 5. The extraction recoveries were not significantly lost for 4 cycles and slightly changed after 5 cycles, as shown in the reusability results shown in Fig. 5. These results suggested that the GO-PANCMA NFs exhibited acceptable reproducibility and reusability with high extraction performance, thus highlighting a cost-effective advantage of the developed GO-PANCMA NFs.

## Method validation

The proposed method, GO-PANCMA NFs SPE-HPLC-DAD, was validated under the optimized conditions to evaluate its analytical performance for the determination of AMX and OTC. This included validating linear equations, linear range, limit of detection (LOD), and limit of quantification (LOQ) to ensure its applicability to real samples. The validation results are summarized in Table 1. The coefficient of determination ($R^2$) for OTC and AMX was 0.9969 and 0.9925, respectively, indicating that the developed approach demonstrated high linearity, as shown in **Figure S3**. The LODs and LOQs were calculated by 3 S/m and 10 S/m, respectively, where S is the standard deviation of the first point in the calibration curve and m is the slope of the regression line[55]. The LODs and LOQs were found to be 1.46 and 4.8 µg/L for OTC and 1.50 µg/L and 5.0 µg/L for AMX, respectively. The results suggest that the developed method enables reliable quantification of the target analytes at the maximum residue levels (MRLs) recommended by the World Health Organization (WHO). Furthermore, the ER% for AMX and OTC was 33.7% and 99.8%, with %RSDs lower than 7. These results indicate that the method not only

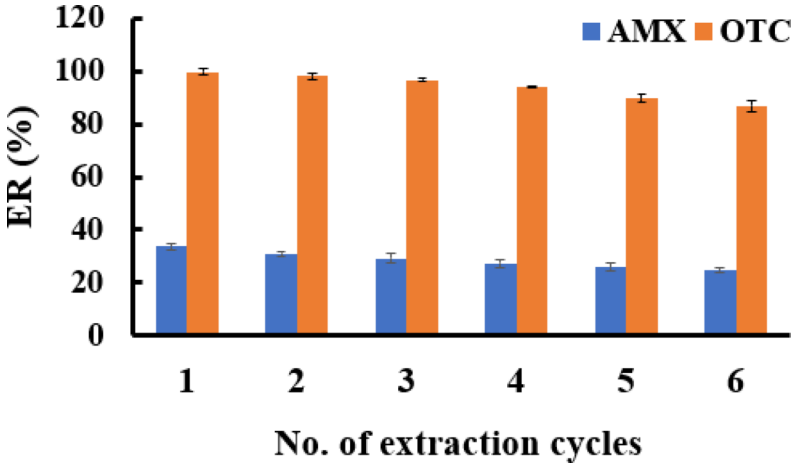


**Fig. 5**. Reusability test of GO-PANCMA NFs. Analytes concentration, 50 µg/L; sample volume,50 ml; sorbent weight, 6 mg; desorption solvent 0.6 ml 0.2 M HCl in MeOH; sample pH, 3; flow rate, 0.83 mL/min.

| Compounds | Linear range (µg/L) | Calibration curves | $R^2$ | LOD (µg/L) | LOQ (µg/L) | RSD (%) | EFs | %ER |
|---|---|---|---|---|---|---|---|---|
| Amoxicillin (AMX) | 5–100 | Y = 0.4777 x + 8.8069 | 0.9925 | 1.50 | 5.0 | < 6 | 21 | 33.7 |
| Oxytetracycline (OTC) | 5–100 | Y = 0.68x-2.9716 | 0.9969 | 1.46 | 4.8 | < 7 | 47 | 99.8 |

**Table 1**. The validation data of SPE-HPLC-DAD.

| | | AMX | | | OTC | | |
|---|---|---|---|---|---|---|---|
| Sample | Spiked (µg/L) | Found (µg/L) | %RR | RSD % | Found (µg/L) | %RR | RSD % |
| *Surface water 1* | 0 | ND* | - | - | ND* | - | - |
| | 40 | 37.69 ± 0.65 | 94.2 | 2.4 | 38.37 ± 0.51 | 95.9 | 2.2 |
| | 80 | 76.25 ± 0.49 | 95.3 | 1.1 | 72.42 ± 2.19 | 90.5 | 4.7 |
| *Surface water 2* | 0 | ND* | - | - | ND* | - | - |
| | 40 | 36.48 ± 0.75 | 91.2 | 2.8 | 37.15 ± 0.59 | 92.8 | 2.7 |
| | 80 | 70.72 ± 1.42 | 88.4 | 3.3 | 70.14 ± 1.50 | 87.6 | 3.4 |
| *Skim milk* | 0 | ND* | - | - | 8.21 ± 0.1 | - | 3.1 |
| | 40 | 38.39 ± 0.75 | 95.9 | 2.8 | 50.72 ± 0.83 | 106.3 | 2.6 |
| | 80 | 79.54 ± 0.30 | 99.4 | 0.7 | 82.13 ± 1.45 | 92.4 | 2.7 |
| *Whole milk* | 0 | ND* | - | - | 10.84 ± 0.1 | - | 1.8 |
| | 40 | 37.49 ± 0.29 | 93.7 | 1.1 | 51.46 ± 0.59 | 101.5 | 1.9 |
| | 80 | 78.14 ± 1.96 | 97.6 | 4.3 | 83.06 ± 1.16 | 90.3 | 2.2 |

**Table 2**. Determination of AMX and OTC in environmental water and milk samples. ND* analytes not detected.

meets the WHO's MRLs for the detection of antibiotics but also demonstrates reliability in quantification with high precision, as evidenced by the good recovery percentages and the low relative standard deviations.

## Real samples analysis

To demonstrate the applicability of the proposed method, the analysis of AMX and OTC in environmental water and food samples was examined and the results are presented in **Figure S4**. Environmental water samples collected from canal and pond in Bangkok, Thailand were used as real samples for environmental application. Furthermore, skim and whole milk were used as food samples. As shown in Table 2, AMX was not detected in either environmental water or milk samples, but OTC was found in milk samples (8.21 µg/L in skim milk and 10.84 µg/L in whole milk) which is lower than the acceptable MRL (100 µg/L) as recommended by FAO/WHO[56]. For testing the accuracy of the method, the spiked samples at 40 and 80 µg/L were examined. The %RR results of AMX and OTC in environmental water and milk samples ranged from 87.6 to 95.9% and 90.3 to 106.3%, respectively. The precision (%RSD) results ranged from 1.1 to 4.7% and from 1.9 to 4.3% for environmental

| Adsorbents | Detection method | Analyte | Sample | LOQ | LOD | %RR | RSD (%) | Reference |
|---|---|---|---|---|---|---|---|---|
| GO-polyethylene terephthalate NFs | μ-SPE-HPLC-UV | Tetracycline, Cefotaxime | Honey | 47.1and 10 μg/kg | 15.3and 3.0 μg/kg | 89–98 | 3.6–5.6 | 53 |
| Activated carbon-polyacrylonitrile (PAN) NFs | DSPE-HPLC-DAD | Ciprofloxacin, Danofloxacin, Enrofloxacin | Surface water | 0.53–2.17 μg/L | 0.05–0.20 μg/L | 90–99 | 3–4 | 60 |
| Polyvinyl alcohol triethoxysilane -$Fe_3O_4$@$SiO_2$ | SPE- UV–VIS | Sulfamethoxazole, Trimethoprim | Surface water | 0.1–50 mg/L | 0.0317–0.247 mg/L | 95.1–98.2 | < 3 | 61 |
| C-nanofiber-coated magnetic nanoparticles | MSPE-HPLC-DAD | Chloramphenicol, Tetracycline | Milk | 9.63 and 9.83 ng/mL | 3.02 and 3.52 ng/mL | 94.6–105.4 | < 4 | 58 |
| Polystyrene-PAN NFs | PFSPE-HPLC-MS/MS | Enrofloxacin, Ciprofloxacin, Ofloxacin | Milk | 0.53 – 1.29 ng/mL | 0.16–0.39 ng/mL | 88.68–97.63 | < 7 | 59 |
| $Fe_3O_4$-GO-Agarose-Chitosan composite | MSPE-HPLC-UV | Streptomycin, Gentamicin | Chicken egg | 0.3–0.6 μg/kg | 0.1–0.19 μg/kg | 94 | 2.5 | 62 |
| Molecularly imprinted $Fe_3O_4$@POSS nanoparticles | MI-MSPE-HPLC-UV | Ofloxacin, Enrofloxacin, Danofloxacin | Milk | 5.84–41.38 ng/ml | 1.76–12.42 ng/mL | 75.6–102.9 | < 11 | 54 |
| GO-PANCMA NFs | SPE-HPLC-DAD | Oxytetracycline, Amoxicillin | Surface water, milk | 4.8–5.0 μg/L | 1.46–1.50 μg/L | 87.6–106.3 | 1.1–4.7 | This study |

**Table 3**. Comparison of GO-PANCMA NFs SPE-HPLC-DAD method with other reported methods for detection of antibiotic residues. μ-SPE, DSPE, MSPE, PFSPE, micro, dispersive, magnetic, packed-fiber solid phase extraction.

water and milk samples, respectively, thus revealing that the developed method holds a substantial potential for the use in the detection of AMX and OTC in environmental water and milk samples.

## Method comparison study

The proposed method, GO-PANCMA NFs SPE-HPLC-DAD, was compared with previously reported techniques for the determination of antibiotic residues in different food matrices and the results are summarized in Table 3. The results of the comparison study showed that in terms of LODs, LOQs, recoveries, and RSDs, this work is comparable and/or better than those obtained by the other methods, thus indicating that the GO-PANCMA-NFs possessed a great potential in sample preparation applications. The LOD of the proposed method was as low as the most sensitive analytical method for antibiotic detection. LODs for OTC and AMX were 1.46 and 1.50 μg/L, respectively, with RSD lower than 5%. Based on the comparison study results shown in Table 3, the developed method has a great advantage over other methods for the detection of antibiotic residues in milk with the minimal organic solvents required. For example, in the current work, organic solvent such as acetonitrile is not required to get rid of protein in milk samples in the sample preparation steps as it was used in other previously reported methods[57–59]. However, the current method used a few drops of concentrated HCl to precipitate protein and to adjust the sample pH condition for extraction in a single step. Overall, the detection of AMX and OTC target analytes via simple and rapid sample preparation process can be an attractive extraction technique for many researchers. This method also shows potential for transferability to other pharmaceutical analytes and sample matrices, particularly those with similar physicochemical properties. Electrospun nanofiber-based sorbents have been applied to a wide range of target compounds in food and environmental monitoring applications due to their high surface area and tunable functional groups. These characteristics make the approach a promising tool for enhancing detection capabilities across various applications. Accordingly, this method could be potential for broader use in monitoring emerging contaminants across diverse sample types, supporting the innovative solutions in analytical chemistry.

## Conclusion

In summary, GO-PANCMA NFs were fabricated with larger average diameters compared to PANCMA NFs. Spectroscopic analyses including XRD, Raman spectroscopy, XPS, and FT-IR confirmed the production of GO-PANCMA NFs. Optimization of SPE conditions were studied including desorption solvent, sample pH, and extraction time. Under the optimal conditions, OTC and AMX exhibited good linearity, low LODs/LOQs, and acceptable %RR ranges from 87.7 to 106.3%, with RSDs below 5.0%. The proposed method, GO-PANCMA NFs SPE-HPLC-DAD, can be applied to different sample matrices effectively with high accuracy and precision. These results underscore the efficacy of the prepared GO-based nanofibers as SPE sorbents in sample preparation for extracting and enriching trace amounts of two antibiotics, AMX and OTC, which belong to two different classes, in milk and environmental water samples. The developed method offers a significant advantage over existing techniques for detecting antibiotic residues in milk. It provides a simple, one-step protein precipitation pretreatment that minimizes the use of organic solvents, making it environmentally friendly. Additionally, the GO-PANCMA NFs can be reused for five times, suggesting a cost-effective and sustainable approach for ongoing analyses.

## Data availability

The datasets used and/or analyzed during the current study are available from the corresponding author on reasonable request.

Received: 26 January 2025; Accepted: 28 April 2025
Published online: 24 May 2025

## References


1. Wang, Y. et al. Antibiotic residues of drinking-water and its human exposure risk assessment in rural Eastern China. *Water Res.* **236**, 119940 (2023).
2. Gai, S. et al. Highly stable Zinc-Based Metal–Organic frameworks and corresponding flexible composites for removal and detection of antibiotics in water. *ACS Appl. Mater. Interfaces*. **12** (7), 8650–8662 (2020).
3. Chen, J., Ying, G. G. & Deng, W. J. Antibiotic residues in food: extraction, analysis, and human health concerns. *J. Agric. Food Chem.* **67** (27), 7569–7586 (2019).
4. Ben, Y. et al. Efficient detection and assessment of human exposure to trace antibiotic residues in drinking water. *Water Res.* **175**, 115699 (2020).
5. Kumar, A., Panda, A. K. & Sharma, N. Determination of antibiotic residues in bovine milk by HPLC-DAD and assessment of human health risks in Northwestern Himalayan region, India. *J. Food Sci. Technol.* **59** (1), 95–104 (2022).
6. Camire, A. et al. Development of electrospun lignin nanofibers for the adsorption of pharmaceutical contaminants in wastewater. *Environ. Sci. Pollut. Res.* **27** (4), 3560–3573 (2020).
7. Wongsuvan, G. et al. Antibiotic use in poultry: a survey of eight farms in Thailand. *Bull. World Health Organ.* **96** (2), 94–100 (2018).
8. Di Stefano, V. & Avellone, G. Food contaminants. *J. Food Stud.* **3** (1), 88–103 (2014).
9. Alanazi, F. et al. Determination of Tetracycline, Oxytetracycline and Chlortetracycline residues in seafood products of Saudi Arabia using high performance liquid chromatography–Photo diode array detection. *Saudi Pharm. J.* **29** (6), 566–575 (2021).
10. Ramatla, T. et al. Evaluation of antibiotic residues in Raw meat using different analytical methods. *Antibiot. (Basel).* **6** (4), 34 (2017).
11. Zhou, J. et al. Covalent organic framework/polyacrylonitrile electrospun nanofiber for dispersive Solid-Phase extraction of trace quinolones in food samples. *Nanomaterials* **12** (14), 2482 (2022).
12. Tahmasebi, E. Adsorption efficiency enhancing of electrospun Polycaprolactone nanofibers towards acidic Polar drugs through the incorporation of a composite of graphene oxide nanosheets and Al(30) polyoxocations: a comparative study. *Analyst* **143** (19), 4684–4698 (2018).
13. Jagirani, M. S. & Soylak, M. A review: recent advances in solid phase Microextraction of toxic pollutants using nanotechnology scenario. *Microchem. J.* **159**, 105436 (2020).
14. Yao, N. et al. Insight into adsorption of combined antibiotic-heavy metal contaminants on graphene oxide in water. *Sep. Purif. Technol.* **236**, 116278 (2020).
15. Soylak, M., Ozalp, O. & Uzcan, F. Magnetic nanomaterials for the removal, separation and preconcentration of organic and inorganic pollutants at trace levels and their practical applications: A review. *Trends Environ. Anal. Chem.* **29**, e00109 (2021).
16. Du, F. et al. Magnetic stir cake sorptive extraction of trace Tetracycline antibiotics in food samples: Preparation of metal-organic framework-embedded polyhipe monolithic composites, validation and application. *Anal. Bioanal. Chem.* **411** (10), 2239–2248 (2019).
17. Pérez-Rodríguez, M. et al. An overview of the main foodstuff sample Preparation technologies for Tetracycline residue determination. *Talanta* **182**, 1–21 (2018).
18. El-Deen, A. K. & Hussain, C. M. Recent developments in green magnetic nanoparticles for extraction and preconcentration of pollutants from environmental samples. *Trends Environ. Anal. Chem.* **39**, e00211 (2023).
19. Amini, A. et al. A porous multifunctional and magnetic layered graphene oxide/3D mesoporous MOF nanocomposite for rapid adsorption of uranium(VI) from aqueous solutions. *J. Ind. Eng. Chem.* **93**, 322–332 (2021).
20. Yola, B. B. et al. A novel electrochemical detection method for butylated hydroxyanisole (BHA) as an antioxidant: a BHA imprinted polymer based on a nickel ferrite@graphene nanocomposite and its application. *Analyst* **148** (16), 3827–3834 (2023).
21. Meriç, Ç. S. et al. Determination of Paclobutrazol using square wave voltammetry based on a molecularly imprinted polymer and boron-doped copper oxide/graphene nanocomposite. *Anal. Methods*. **17** (5), 1080–1089 (2025).
22. Wang, H. B. et al. Development of rapid and Label-Free fluorescence sensing of tetracyclines in milk based on Poly(Adenine) DNA-Templated Au nanoclusters. *Food. Anal. Methods*. **11** (11), 3095–3102 (2018).
23. Li, X. et al. Recycling and reutilizing polymer waste via electrospun micro/nanofibers: A review. *Nanomaterials (Basel).* **12** (10), 1663 (2022).
24. Aliabadi, M. et al. Electrospun nanofiber membrane of PEO/Chitosan for the adsorption of nickel, cadmium, lead and copper ions from aqueous solution. *Chem. Eng. J.* **220**, 237–243 (2013).
25. Weng, R. et al. Electrospun graphene Oxide–Doped Nanofiber-Based solid phase extraction followed by High-Performance liquid chromatography for the determination of Tetracycline antibiotic residues in food samples. *Food. Anal. Methods*. **12** (7), 1594–1603 (2019).
26. Turan, H. E. et al. Graphene quantum Dots incorporated NiAl2O4 nanocomposite based molecularly imprinted electrochemical sensor for 5-hydroxymethyl furfural detection in coffee samples. *Anal. Methods*. **15** (15), 1932–1938 (2023).
27. Deveci, H. A. et al. Bisphenol A imprinted electrochemical sensor based on graphene quantum Dots with Boron functionalized g-C3N4 in food samples. *Biosensors* **13** https://doi.org/10.3390/bios13070725 (2023).
28. Feng, Z. Q., Yuan, X. & Wang, T. Porous polyacrylonitrile/graphene oxide nanofibers designed for high efficient adsorption of chromium ions (VI) in aqueous solution. *Chem. Eng. J.* **392**, 123730 (2020).
29. Lee, J. et al. Electrospun PAN–GO composite nanofibers as water purification membranes. *J. Appl. Polym. Sci.* **135** (7), 45858 (2017).
30. Chen, D., Feng, H. & Li, J. Graphene oxide: preparation, functionalization, and electrochemical applications. *Chem. Rev.* **112** (11), 6027–6053 (2012).
31. Khajeh, M. & Barkhordar, A. Fe3O4/Graphene oxide composite for adsorption of methylene blue and Methyl orange in water treatment. *J. Appl. Spectrosc.* **87** (4), 701–707 (2020).
32. Seidi, S. et al. Synthesis and characterization of polyamide-graphene oxide-polypyrrole electrospun nanofibers for spin-column micro solid phase extraction of Parabens in milk samples. *J. Chromatogr. A*. **1599**, 25–34 (2019).
33. Marcano, D. C. et al. Improved synthesis of graphene oxide. *ACS Nano*. **4** (8), 4806–4814 (2010).
34. Du, F., Alam, M. N. & Pawliszyn, J. Aptamer-functionalized solid phase microextraction–liquid chromatography/tandem mass spectrometry for selective enrichment and determination of thrombin. *Anal. Chim. Acta*. **845**, 45–52 (2014).
35. Arabsorkhi, B. & Sereshti, H. Determination of Tetracycline and cefotaxime residues in honey by micro-solid phase extraction based on electrospun nanofibers coupled with HPLC. *Microchem. J.* **140**, 241–247 (2018).
36. Allafchian, A. R. & Jalali, S. A. H. Synthesis, characterization and antibacterial effect of poly(acrylonitrile/maleic acid)–silver nanocomposite. *J. Taiwan Inst. Chem. Eng.* **57**, 154–159 (2015).
37. Rostami, M. et al. Polycaprolactone/polyacrylic acid/graphene oxide composite nanofibers as a highly efficient sorbent to remove lead toxic metal from drinking water and Apple juice. *Sci. Rep.* **14** (1), 4372 (2024).
38. Tripathy, M. & Hota, G. Maghemite and graphene oxide embedded polyacrylonitrile electrospun nanofiber matrix for remediation of arsenate ions. *ACS Appl. Polym. Mater.* **2** (2), 604–617 (2019).

39. Barus, D. A. et al. Enhanced adsorption performance of Chitosan/cellulose nanofiber isolated from Durian Peel waste/graphene oxide nanocomposite hydrogels. *Environ. Nanatechnol. Monit. Manage.* **17**, 100650 (2022).
40. Zhang, L. et al. Electrospun Titania nanofibers segregated by graphene oxide for improved visible light photocatalysis. *Appl. Catal. B*. **201**, 470–478 (2017).
41. Wang, S. D. et al. Improving antibacterial activity and biocompatibility of bioinspired electrospinning silk fibroin nanofibers modified by graphene oxide. *ACS Omega*. **3** (1), 406–413 (2018).
42. Swaminathan, S., Muthumanickkam, A. & Imayathamizhan, N. M. An effective removal of methylene blue dye using polyacrylonitrile yarn waste/graphene oxide nanofibrous composite. *Int. J. Environ. Sci. Technol.* **12** (11), 3499–3508 (2014).
43. Abd-Elhamid, A. I. et al. *Fabrication of polyacrylonitrile/β-cyclodextrin/graphene Oxide Nanofibers Composite as an Efficient Adsorbent for Cationic Dye* 11p. 100207 (Environmental Nanotechnology, Monitoring & Management, 2019).
44. Liu, Q. et al. Synthesis of Fe3O4/Polyacrylonitrile composite electrospun nanofiber mat for effective adsorption of Tetracycline. *ACS Appl. Mater. Interfaces*. **7** (27), 14573–14583 (2015).
45. Wang, J. et al. One-Step Preparation of graphene oxide/cellulose nanofibril hybrid aerogel for adsorptive removal of four kinds of antibiotics. *J. Nanomaterials*. **2017**, 5150613 (2017).
46. Liang, W. et al. Hydrophobic polyacrylonitrile membrane Preparation and its use in membrane contactor for CO2 absorption. *J. Membr. Sci.* **569**, 157–165 (2019).
47. Sun, Y. et al. One pot synthesis of magnetic graphene/carbon nanotube composites as magnetic dispersive solid-phase extraction adsorbent for rapid determination of Oxytetracycline in sewage water. *J. Chromatogr. A*. **1422**, 53–59 (2015).
48. Ma, N. et al. Determination of tetracyclines in chicken by dispersive solid phase Microextraction based on Metal-Organic frameworks/molecularly imprinted Nano-polymer and ultra performance liquid chromatography. *Food. Anal. Methods*. **13** (5), 1211–1219 (2020).
49. Komal et al. Amelioration of adsorptive efficacy by synergistic assemblage of functionalized graphene oxide with esterified cellulose nanofibers for mitigation of pharmaceutical waste. *J. Hazard. Mater.* **424**, 127541 (2022).
50. Nguyen, V. T. et al. Antibiotics Tetracycline adsorption and flame-retardant capacity of eco-friendly aerogel-based nanocellulose, graphene oxide, Polyvinyl alcohol, and sodium bicarbonate. *J. Environ. Chem. Eng.* **11** (2), 109523 (2023).
51. Gao, Y. et al. Adsorption and removal of Tetracycline antibiotics from aqueous solution by graphene oxide. *J. Colloid Interface Sci.* **368** (1), 540–546 (2012).
52. Yao, Q. et al. 3D assembly based on 2D structure of cellulose nanofibril/graphene oxide hybrid aerogel for adsorptive removal of antibiotics in water. *Sci. Rep.* **7** (1), 45914 (2017).
53. Arabsorkhi, B. & Sereshti, H. Determination of Tetracycline and cefotaxime residues in honey by micro-solid phase extraction based on electrospun nanofibers coupled with HPLC. *Microchem. J.* **140**, (2018).
54. He, H. B. et al. Fabrication of Enrofloxacin imprinted organic-inorganic hybrid mesoporous sorbent from nanomagnetic polyhedral oligomeric silsesquioxanes for the selective extraction of fluoroquinolones in milk samples. *J. Chromatogr. A*. **1361**, 23–33 (2014).
55. Pengsomjit, U. et al. Graphene-based gel electromembrane extraction coupled with modified screen-printed carbon electrode for detecting streptomycin in honey samples: greener strategy for food analysis. *Talanta* **268**, 125334 (2024).
56. Joint, F. et al. *Residues of some Veterinary Drugs in Animals and foods / monographs Prepared by the Sixtieth Meeting of the Joint FAO/WHO Expert Committee on Food Additives, Geneva, 6–12 February 2003* (World Health Organization: Geneva, 2003).
57. Qiu, Q. et al. Porous electrospun microfibers for low flow-resistant solid phase extraction of fluoroquinolones in tap water, egg and milk samples. *J. Chromatogr. A*. **1661**, 462719 (2022).
58. Vuran, B. et al. Determination of Chloramphenicol and Tetracycline residues in milk samples by means of nanofiber coated magnetic particles prior to high-performance liquid chromatography-diode array detection. *Talanta* **230**, 122307 (2021).
59. Wei, L. et al. Simultaneous determination of nine quinolones in pure milk using PFSPE-HPLC-MS/MS with PS-PAN nanofibers as a sorbent. *Foods* **11** https://doi.org/10.3390/foods11131843 (2022).
60. Mogolodi Dimpe, K. & Nomngongo, P. N. Application of activated carbon-decorated polyacrylonitrile nanofibers as an adsorbent in dispersive solid-phase extraction of fluoroquinolones from wastewater. *J. Pharm. Anal.* **9** (2), 117–126 (2019).
61. Mehrabi, F. et al. Magnetic solid phase extraction based on PVA - TEOS / grafted Fe3O4@SiO2 magnetic nanofibers for analysis of sulfamethoxazole and Trimethoprim in water samples. *J. Solid State Chem.* **292**, 121716 (2020).
62. Sajjad, M. et al. Magnetic solid phase extraction of aminoglycosides residue in chicken egg samples using Fe3O4-GO-Agarose-Chitosan composite. *Food Chem.* **430**, 137092 (2024).


## Acknowledgements

This work is funded by the Second Century Fund, Chulalongkorn University (C2 F), PhD Scholarship. The authors extend their appreciation to the Researchers Supporting Project number (RSPD2025R944), King Saud University, Riyadh, Saudi Arabia for funding this work.

## Author contributions

S. A. M.: Investigation, Methodology, Experiments designation, Formal analysis, Data curation, Writing - original draft, Writing - review & editing. W. A.: Conceptualization, Visualization, Data curation, Validation, Writing - review & editing. I. A. D.: Project administration, Funding acquisition, Writing - review & editing. M. A. S. A.: Project administration, Funding acquisition, Writing - review & editing. P. V.: Conceptualization, Data curation, Visualization, Methodology, Writing - review & editing, Supervision, Project administration.

## Declarations

## Competing interests

The authors declare no competing interests.

## Additional information

**Supplementary Information** The online version contains supplementary material available at https://doi.org/10.1038/s41598-025-00356-0.

**Correspondence** and requests for materials should be addressed to P.V.

**Reprints and permissions information** is available at www.nature.com/reprints.